OXFORD

REGULAR RESEARCH ARTICLE

LiCl Pretreatment Ameliorates Adolescent Methamphetamine Exposure-Induced Long-Term Alterations in Behavior and Hippocampal Ultrastructure in Adulthood in Mice

Peng Yan, Dan Xu, Yuanyuan Ji, Fangyuan Yin, Jingjing Cui, Rui Su, Yunpeng Wang, Yongsheng Zhu, Shuguang Wei, Jianghua Lai

College of Forensic Science, Xi'an Jiaotong University, Xi'an, Shaanxi, People's Republic of China (Drs Yan, Ji, Yin, Cui, Su, Wang, Zhu, Wei, and Lai); Traditional Chinese Medicine Department, Shenyang Pharmaceutical University, Shenyang, Liaoning, People's Republic of China (Dr Xu); Key Laboratory of Forensic Science, National Health and Family Planning Commission, Xi'an, Shaanxi, People's Republic of China (Drs Wei and Lai).

Correspondence: Shuguang Wei, PhD, College of Forensic Science, Xi'an Jiaotong University, 76 Yanta West Road, Xi'an 710061, People's Republic of China (weisg@mail.xjtu.edu.cn); and Jianghua Lai, PhD, College of Forensic Science, Xi'an Jiaotong University, 76 Yanta West Road, Xi'an 710061, People's Republic of China (laijh1011@mail.xjtu.edu.cn).

Abstract

Background: Adolescent methamphetamine exposure causes a broad range of neurobiological deficits in adulthood. Glycogen synthase kinase-3β is involved in various cognitive and behavioral processes associated with methamphetamine exposure. This study aims to investigate the protective effects of the glycogen synthase kinase-3β inhibitor lithium chloride on adolescent methamphetamine exposure-induced long-term alterations in emotion, cognition, behavior, and molecule and hippocampal ultrastructure in adulthood.
Methods: A behavioral test battery was used to investigate the protective effects of lithium chloride on adolescent methamphetamine exposure-induced long-term emotional, cognitive, and behavioral impairments in mice. Western blotting and immunohistochemistry were used to detect glycogen synthase kinase-3β activity levels in the medial prefrontal cortex and dorsal hippocampus. Electron microscopy was used to analyze changes in synaptic ultrastructure in the dorsal hippocampus. Locomotor sensitization with a methamphetamine (1 mg/kg) challenge was examined 80 days after adolescent methamphetamine exposure.
Results: Adolescent methamphetamine exposure induced long-term alterations in locomotor activity, novel spatial exploration, and social recognition memory; increases in glycogen synthase kinase-3β activity in dorsal hippocampus; and decreases in excitatory synapse density and postsynaptic density thickness in CA1. These changes were ameliorated by lithium chloride pretreatment. Adolescent methamphetamine exposure-induced working memory deficits in Y-maze spontaneous alternation test and anxiety-like behavior in elevated-plus maze test spontaneously recovered after long-term methamphetamine abstinence. No significant locomotor sensitization was observed after long-term methamphetamine abstinence.
Conclusions: Hyperactive glycogen synthase kinase-3β contributes to adolescent chronic methamphetamine exposure-induced behavioral and hippocampal impairments in adulthood. Our results suggest glycogen synthase kinase-3β may be a potential target for the treatment of deficits in adulthood associated with adolescent methamphetamine abuse.

Significance Statement

Current methamphetamine (METH)-related studies tend to focus on adults, ignoring adolescent drug exposure. This study investigated the protective effects of the GSK3β inhibitor lithium chloride (LiCl) on adolescent METH exposure-induced long-term alterations in emotion, cognition, behavior, and hippocampal ultrastructure. Adolescent METH exposure significantly increased GSK3β activity in the medial prefrontal cortex (mPFC) and dorsal hippocampus (dHIP), but this effect persisted only in the dHIP in adulthood. Treatment with LiCl before METH administration prevented adolescent METH exposure-induced long-term behavioral alterations, including mild hyperactivity, reduced novel spatial exploration, and impaired social recognition memory as well as GSK3β hyperactivity and ultrastructural alterations in the dHIP in adulthood. Adolescent METH exposure-induced working memory deficits in the Y-maze spontaneous alternation test and anxiety-related behavior in the elevated-plus maze test spontaneously recovered after long-term METH abstinence. Thus, our data suggest GSK3β may be a potential target to improve adolescent METH exposure-induced long-term behavioral and hippocampal impairments.

Introduction

Methamphetamine (METH) is a widely abused psychostimulant with long-lasting neurobiological consequences (Moszczynska and Callan, 2017). Adolescence is a sensitive, vulnerable period for the effects of drug use, and the prevalence of chronic METH use among teenagers is increasing and occurring at earlier ages (Spear, 2016; UNODC, 2017). However, current METH-related studies tend to focus on adult populations, ignoring adolescent drug exposure (Luikinga et al., 2018). Thus, studying how adolescent METH exposure affects emotion, cognition, and behavior in the both adolescence and adulthood is necessary and important.

Previous adolescent studies on the neurotoxic effects of METH tend to focus on brain regions that are associated with dopaminergic reward pathways (Buck and Siegel, 2015). An increasing number of studies have demonstrated that the medial prefrontal cortex (mPFC) and hippocampus are sensitive to adolescent drug exposure-induced nerve damage (Smith, 2003; Spear, 2016; Renard et al., 2017; Luikinga et al., 2018). However, very few studies have reported on the long-term consequence of adolescent METH exposure on the mPFC, hippocampus, and related behaviors. Vorhees et al. suggested that METH exposure in postnatal day (PND) 41 to 50 rats significantly impairs spatial learning/reference memory and sequential learning, indicating impaired mPFC and hippocampal functions in adulthood (PND 80) (Vorhees et al., 2005). In another study in adolescent mice exposed to METH on PND 28 to 42, at 21 days after the last METH administration, mice exhibited a decrease in hippocampal plasticity, which was not observed 23 hours after the last METH injection (North et al., 2013). In addition, the PFC and hippocampus show a biphasic pattern in volume changes across adolescence, and adolescent METH exposure may disorganize the normal pattern of growth and maturation in these brain regions and result in long-term neurobiological alterations (Wierenga et al., 2014; Jalbrzikowski et al., 2017). This evidence highlights the need for further research to uncover the long-term effects of adolescent METH exposure on the mPFC and hippocampus.

Glycogen synthase kinase-3 (GSK3β) is a key regulator in neurodevelopmental and neuronal plasticity and a master downstream mediator in phosphoinositide-3-OH kinase/Akt pathway and canonical Wnt pathway, which play crucial roles in METH dependence (Chen et al., 2007; Kishimoto et al., 2008; Salcedo-Tello et al., 2011). Moreover, increased GSK3β activity is implicated in METH-induced hyperactivity, locomotor sensitization, and neurotoxicity (Xu et al., 2011; Wang et al., 2012; Wu et al., 2015; Xing et al., 2015). The GSK3β inhibitor lithium is one of the most common prescription medicines for the treatment of bipolar disorder and has neuroprotective effects (Klein and Melton, 1996; Phiel and Klein, 2001; King et al., 2014). Lithium treatment ameliorates METH-induced neurotoxicity in vitro and METH-induced locomotor sensitization in vivo (Xu et al., 2011; Wu et al., 2015). However, thus far, the effectiveness of lithium on long-term changes in nerve and behavior following adolescent METH exposure remains unknown.

Therefore, in the present study, we aimed to investigate the possible protective effects of lithium chloride (LiCl) on adolescent METH exposure-induced long-term emotional, cognitive, behavioral, molecular, and ultrastructural alterations in adulthood.

MATERIALS AND METHODS

Study Design

Experiment 1: Effects of METH Exposure on GSK3β Activity in the mPFC and Dorsal Hippocampus (dHIP) in Adolescence

Adolescent mice were randomly divided into the saline and chronic METH groups (n = 12 per group) and received 1 daily (o.d.) i.p. injection of METH (1 mg/kg) or saline (10 mL/kg) for 7 days from PND 45 to 51. The dose selection for the drugs was based on a previous study demonstrating that METH treatment at a dose of 1 mg/kg in mice for 7 days impairs recognition memory (Kamei et al., 2006). Twenty-four hours after the last METH or saline injection, mice were killed by decapitation, and the mPFC and dHIP were extracted to determine GSK3β activity by western blotting. Adolescence in *Mus musculus* is defined as the period from PND 22 to PND 60 (Brust et al., 2015; Spear, 2016). An overview of the experimental timing is provided in Figure 1 (Experiment 1).

Experiment 2: Effects of LiCl Pretreatment on METH Exposure-Induced Increased GSK3β Activity in the mPFC and dHIP in Adolescence

Adolescent mice were randomly divided into the following groups (n = 10 per group): saline × saline, LiCl × saline, saline
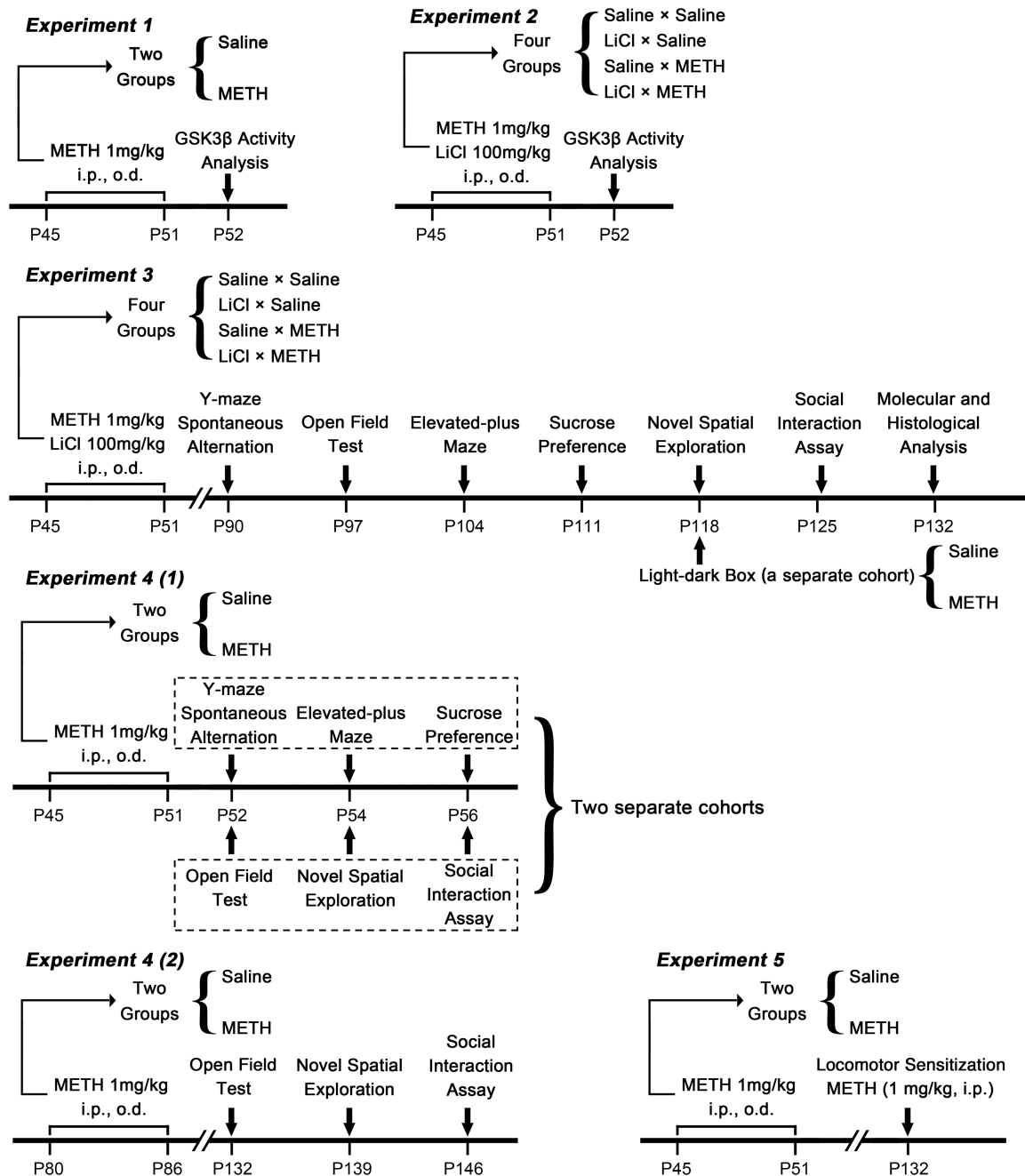
Figure 1. Overview of experimental time courses.

× METH, and LiCl × METH. In each group, daily METH (1 mg/kg, i.p., o.d.) or saline (10 mL/kg, i.p., o.d.) administration 30 minutes after LiCl (100 mg/kg, i.p., o.d.) or saline (10 mL/kg, i.p., o.d.) injection was carried out for 7 days from PND 45 to 51. The LiCl dose and interval were chosen based on studies showing that this dose inhibits METH exposure-induced increases in GSK3β activity (Beaulieu et al., 2004; Xu et al., 2011). The day after the last drug administration, mice were killed by decapitation, and the mPFC and dHIP were extracted to determine GSK3β activity by western blotting. An overview of the experimental timing is provided in Figure 1 (Experiment 2).

Experiment 3: Effects of LiCl Pretreatment on Adolescent METH Exposure-Induced Long-Term Emotional, Cognitive, Behavioral and Ultrastructural Alterations in Adulthood

Adolescent mice were also randomly divided into the following groups (n = 14 per group): saline × saline, LiCl × saline, saline × METH, and LiCl × METH. Drug administration in each group was the same as that in Experiment 2. Following a 38-day drug-free period, a behavioral test battery was initiated on PND 90 to investigate the protective effects of LiCl on adolescent METH exposure-induced long-term emotional, cognitive, and behavioral impairments in adulthood. In view of each mouse

participating in multiple behavioral tests, a total of 6 mild, non-invasive behavioral tests were selected to form the behavioral test battery, which was performed in the following sequence: Y-maze spontaneous alternation test for detecting spatial working memory, open field test (OFT) for detecting locomotor activity, elevated-plus maze (EPM) test for detecting anxiety-related behavior, sucrose preference test (SPT) for detecting anhedonia-like behavior, novel spatial exploration test for detecting novel spatial exploration behavior, and social interaction assay for detecting sociability and social recognition memory. To decrease carryover effects from prior tests, we allowed mice to rest for several days between each test. On PND 132, mice were killed, and their brains were harvested for further western blotting, immunohistochemical, and ultrastructural analyses. To investigate the effect of anxiety levels on our novel spatial exploration test, we randomly divided a separate cohort of adolescent mice into the saline and chronic METH groups (n = 8 per group), and drug administration in each group was the same as that in Experiment 1. On PND 118, all mice were subjected to a light-dark box test. An overview of the experimental timing is provided in Figure 1 (Experiment 3).

Experiment 4(1).—Effects of METH Exposure on Emotion, Cognition, and Behavior in Adolescence

Two separate cohorts of adolescent mice were used. Each cohort was randomly divided into the saline and METH groups (n = 10 per group), and drug administration in each group was the same as that in Experiment 1. Behavioral tests were performed after METH exposure in adolescence. One cohort was subjected to the Y-maze spontaneous alternation test, EPM test, and SPT. The other cohort was subjected to the OFT, novel spatial exploration test, and social interaction assay [Figure 1, Experiment 4(1)].

Experiment 4(2).—Effects of Adult METH Exposure on the Locomotor Activity, Novel Spatial Exploration, and Social Interaction after Long-Term METH Abstinence

Adult mice received METH (1 mg/kg, i.p., o.d) or saline (10 ml/kg, i.p., o.d.) (n = 10 per group) for 7 days from PND 80 to 86. All animals were subjected to the OFT, novel spatial exploration test, and social interaction assay on PND 132, 139, and 146, respectively [Figure 1, Experiment 4(2)].

Experiment 5: Effects of Adolescent METH Exposure on the Expression of METH-Induced Locomotor Sensitization in Adulthood

Adolescent mice were randomly divided into the saline and METH groups (n = 8 per group). Drug administration in each group was the same as that in Experiment 1. On PND 132, the possible expression of METH-induced locomotor sensitization was investigated (Figure 1, Experiment 5).

Animals

All animal procedures were conducted according to the NIH Guide for the Care and Use of Laboratory Animals and were approved by the Institutional Animal Care and Use Committee of Xi'an Jiaotong University. Adolescent male C57BL/6J mice were obtained at PND 30 and were maintained with unrestricted access to food and water on a 12-hour-light cycle, and experiments were conducted during the light portion.

Drug Preparation and Administration

METH hydrochloride and LiCl were dissolved in 0.9% saline to a final concentration of 0.1 and 10 mg/mL, respectively. All drugs were freshly prepared before use.

Behavioral Tests

Y-Maze Spontaneous Alternation (Spatial Working Memory)
Mice were randomly placed at the end of one of the 3 arms to avoid placement bias and allowed to freely explore the Y-maze for 5 minutes. Spontaneous alternation (%), total arm entries, and total distance were measured.

OFT (Locomotor Activity)
Exploration of an open field arena was assessed during a 60-minute test. The center area and 4 corner areas were marked by using Any-maze 5.2 software (Stoelting Co., Wood Dale, IL). The distance moved, movement duration, and movement in the center 4 four corners were measured.

EPM (Anxiety-Related Behavior)
Mice were allowed to freely explore the apparatus for 5 minutes. The time spent in open arms (%), entries in open arms (%), head dips, total distance, and total arm entries were measured.

SPT (Anhedonia-Like Behavior)
Mice were given a 2-bottle choice (one with a 1% sucrose solution and another with tap water) for 3 days. Sucrose preference (%) and liquid ingested (mL/g) in the third day of the SPT were analyzed.

Novel Spatial Exploration Test
The procedure for this test was adapted from Melnikova et al. and Wolf et al. (Melnikova et al., 2006; Wolf et al., 2016). This test was conducted in the same Y-maze (spontaneous alternation test apparatus) rotated by 45° with different distal cues. The wall of 1 of the 3 arms was marked with a black and white pattern, which was defined as the novel arm. This test had 2 phases with a 5-minute intertrial interval. During the T1 phase, the novel arm was blocked, and the mice were allowed to freely explore the Y-maze for 5 minutes. During the T2 phase (a second 5-min exploration), the novel arm was opened. The time spent in the novel arm (%), entries in the novel arm (%), latency to first entry, longest single visit to the novel arm, total arm entries, and distance moved were measured. The apparatus and placements of mice for this test are shown in supplementary Figure 1A.

Light and Dark Box (Anxiety-Related Behavior)
Mice were placed in the center of the light chamber and allowed to freely explore the apparatus for 5 minutes. The time spent in the light chamber (%), the number of total transitions, and the total distance were measured.

Social Interaction Assay
The test apparatus was rectangular and 3-chambered. Mice were placed in the central chamber to habituate to the box for 5 minutes, followed by 2 successive test phases with a 5-minute intertrial interval. In the T1 phase (sociability test), an unfamiliar mouse (stranger) was placed in 1 of the 2 lateral chambers and enclosed in a circular acrylic cage. Another empty cage of the same design was placed in the other lateral chamber. Mice were allowed to freely explore the test apparatus for 10 minutes. In the T2 phase (social recognition memory test) (a second 10-minute exploration), a second unfamiliar mouse (novel) was placed in the circular acrylic cage that was empty in the T1 phase. The sociability scores, time in the stranger chamber (%), entries in the stranger chamber (%), social recognition scores, time in the novel chamber (%), entries in the novel chamber (%), total lateral chamber entries, and distance moved were measured. The

apparatus and placements of mice for this test are shown in supplementary Figure 1B.

Locomotor Sensitization

The locomotor sensitization was examined as previously described (Good and Radcliffe, 2011). On PND 132, mice were challenged with METH (1 mg/kg, i.p.), and their activities were recorded immediately for 120 minutes.

Molecular and Histological Analyses

Western Blotting Analyses

GSK3β activity depends on site-specific phosphorylation. Phosphorylation of Tyr216 (Y216) on GSK3β activates GSK3β, whereas phosphorylation of Ser9 (S9) on GSK3β inhibits its activity. Thus, the increased ratio of Y216-phosphorylated GSK3β (pGSK3β-Y216) to total GSK3β (t-GSK3β) and/or the expression level of pGSK3β-Y216 imply increased GSK3β activity. In contrast, the increased ratio of S9-phosphorylated GSK3β (pGSK3β-S9) to t-GSK3β and/or the expression level of pGSK3β-S9 imply decreased GSK3β activity. The western-blotting procedure was conducted as described in our previous study (Wang et al., 2017). The dilutions of primary antibodies were as follows: phosphorylated pGSK3β-Y216 (1:1000), pGSK3β-Ser9 (1:1000), t-GSK3β (1:2000), and GAPDH (internal control, 1:2000). All species-appropriate horseradish peroxidase-conjugated secondary antibodies were used at a dilution of 1:10 000.

Immunohistochemistry

Following anesthetization with 10% chloral hydrate, mice were perfused transcardially with saline, followed by 4% paraformaldehyde in 0.1 M phosphate buffer. Brains were postfixed in 4% paraformaldehyde for 3 hours. After cryopreserving in 30% sucrose, brains were sectioned on a freezing microtome at 30 μm. Immunohistochemical staining was performed according to the manufacturer's protocol using Biotin-Streptavidin HRP Detection Systems (SP-9001, ZSGB-BIO, Beijing, China). The dilution of rabbit anti-phospho-GSK3β-Ser9 was 1:100. The integrated optical density in the mPFC, CA1, CA3, and dentate gyrus (DG) were evaluated.

Electron Microscopic Analysis

Following anesthetization with 10% chloral hydrate, mice were perfused transcardially with saline, followed by 0.1 M phosphate buffer (pH 7.4) containing 4% paraformaldehyde and 0.25% glutaraldehyde. Next, brains were immediately removed and stored in 0.1 M phosphate buffer (pH 7.4) with 4% paraformaldehyde and 2.5% glutaraldehyde at 4°C. The dHIP subregions CA1, CA3, and DG were extracted and dissected into ~1 mm³ pieces. Electron microscopy was conducted as described in a previous report (Tian et al., 2009). The thickness of the postsynaptic density (PSD) at the thickest part, the width of the synaptic cleft, the length of the active zone, and the number of Gray's type-1 asymmetric synapses (excitatory synapses) were measured. More than 60 randomly chosen asymmetric synapses per subregion were analyzed.

Statistical Analysis

Statistical analyses were conducted using GraphPad Prism 7.0 (GraphPad Software Inc., La Jolla, CA). The results are presented as the mean ± SEM. The parametric tests were applied when normality and homogeneity of variance assumptions were satisfied; otherwise the nonparametric tests were used (Mann-Whitney or Kruskal-Wallis). Kruskal-Wallis was followed by Dunn's post hoc test where appropriate. For parametric tests, METH exposure, LiCl pretreatment, and test time were considered independent effects and were analyzed accordingly; that is, when there was only one effect, unpaired t tests were used and when there were 2 or 3 effects, 2- or 3-way ANOVA was used to determine main effects of METH exposure, LiCl pretreatment, or test time and interaction between these effects. Only when there was a statistical interaction were between-group comparisons done (Bonferroni's post hoc test). Differences were defined as statistically significant at $P < .05$.

Detailed methods are provided in Supplementary Materials.

RESULTS

Experiment 1: METH Exposure Significantly Increased GSK3β Activity in the mPFC and dHIP in Adolescent Mice

Based on a comparison of adolescent METH-exposed and saline-treated mice, western-blot analysis revealed that the ratio of pGSK3β-Y216 to t-GSK3β was increased in the dHIP ($t_{(22)} = 2.191$, $P < .05$) (Figure 2F) but not in mPFC (Figure 2B); the ratio of pGSK3β-Ser9 to t-GSK3β was decreased in both the mPFC ($t_{(22)} = 2.698$, $P < .05$) (Figure 2C) and dHIP ($t_{(22)} = 3.142$, $P < .01$) (Figure 2G); and the expression level of t-GSK3β was unchanged in both the mPFC (Figure 2D) and dHIP (Figure 2H) after 7 days of METH exposure.

Experiment 2: LiCl Pretreatment Inhibited the METH Exposure-Induced Increase in GSK3β Activity in the mPFC and dHIP in Adolescence

Two-way ANOVA for the western-blot data of the ratios of pGSK3β-Y216 to t-GSK3β in dHIP (Figure 3F) and pGSK3β-Ser9 to t-GSK3β in mPFC (Figure 3C) and dHIP (Figure 3G) revealed a significant effect of the interaction of METH exposure × LiCl pretreatment ($F_{(1,34)} = 4.287$, $P < .05$; $F_{(1,34)} = 4.912$, $P < .05$; $F_{(1,34)} = 4.558$, $P < .05$), METH exposure ($F_{(1,34)} = 5.025$, $P < .05$; $F_{(1,34)} = 9.141$, $P < .01$; $F_{(1,34)} = 10.01$, $P < .01$), and LiCl pretreatment ($F_{(1,34)} = 4.809$, $P < .05$; $F_{(1,34)} = 12.86$, $P < .01$; $F_{(1,34)} = 7.309$, $P < .05$). Bonferroni's post hoc tests revealed that pretreatment with LiCl inhibited the METH exposure-induced increase in the ratio of pGSK3β-Y216 to t-GSK3β in the dHIP (Figure 3F) and the decrease in the ratio of pGSK3β-Ser9 to t-GSK3β in the mPFC (Figure 3C) and dHIP (Figure 3G).

Experiment 3

LiCl Pretreatment Prevented Adolescent METH Exposure-Induced Mild Hyperactivity, Reduced Novel Spatial Exploration, and Impaired Social Recognition Memory in Adulthood
In this section, we report only the most relevant results that are important for the interpretation of the behavioral changes, and the others are shown in supplementary Table 1.

First, all the tested animals showed similar characteristics in the Y-maze spontaneous alternation test (Figure 4A; supplementary Table 1).

For the OFT, 2-way ANOVA for the data of total distance traveled revealed a significant effect of the interaction of METH exposure × LiCl pretreatment ($F_{(1,51)} = 4.309$, $P < .05$), METH exposure ($F_{(1,51)} = 6.633$, $P < .05$), and LiCl pretreatment ($F_{(1,51)} = 4.689$, $P < .05$). Bonferroni's post hoc tests revealed that, in adulthood, adolescent METH-exposed mice (saline × METH) were markedly
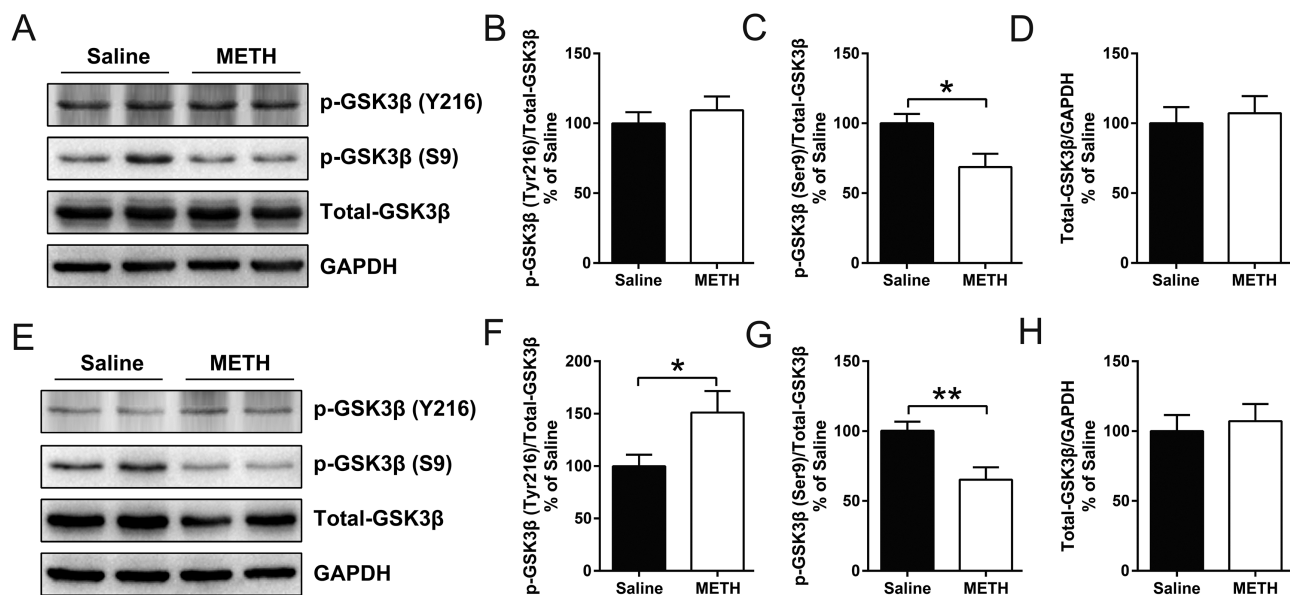
Figure 2. Methamphetamine (METH) exposure during adolescence regulated glycogen synthase kinase 3 beta (GSK3β) phosphorylation patterns and increased GSK3β activity in the medial prefrontal cortex (mPFC) and dorsal hippocampus (dHIP). Representative immunoblot images for mPFC are shown in A. Compared with the control, METH exposure did not alter the ratio of pGSK3β-Y216 to t-GSK3β (B) but decreased the ratio of pGSK3β-S9 to t-GSK3β (C) in the adolescent mPFC, with no significant changes in the relative expression of t-GSK3β (D). Representative immunoblot images for dHIP are shown in E. Compared with the control, METH exposure increased the ratio of pGSK3β-Y216 to t-GSK3β (F) and decreased the ratio of pGSK3β-S9 to t-GSK3β (G) in the adolescent dHIP, with no significant changes in the relative expression of t-GSK3β (H). Data are expressed as the mean ± SEM; n = 12/group; *$P < .05$ and **$P < .01$, comparison between the 2 indicated groups; unpaired t tests.
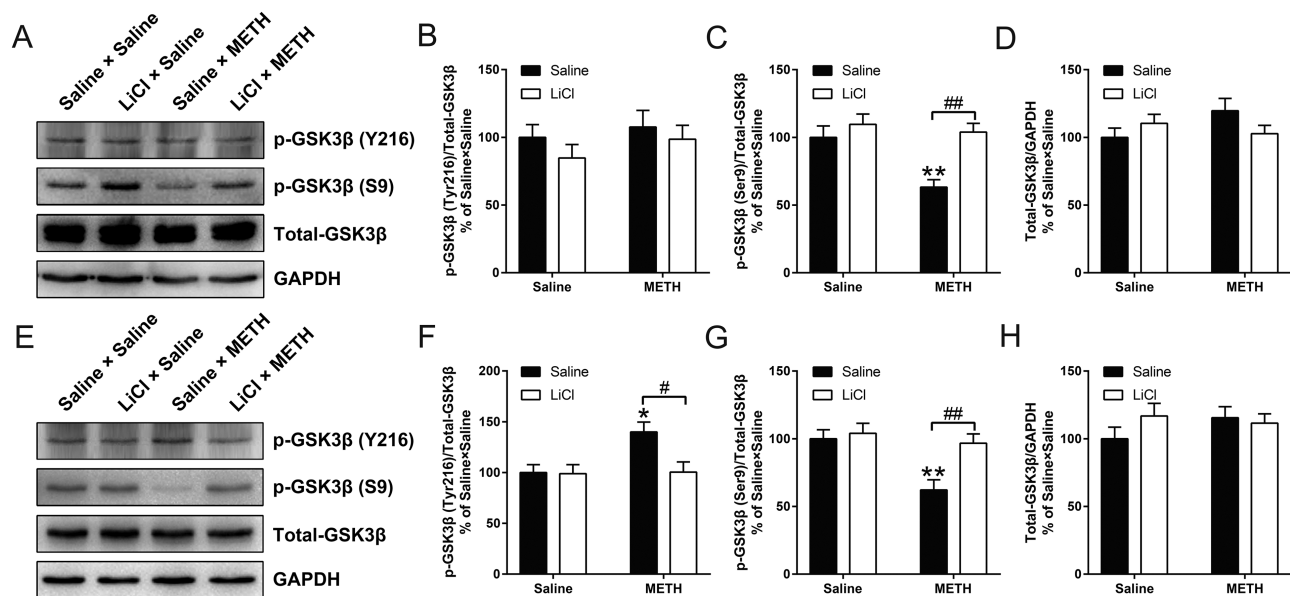

Figure 3. Lithium chloride (LiCl) pretreatment inhibited methamphetamine (METH) exposure-induced increases in glycogen synthase kinase 3 beta (GSK3β) activity in the medial prefrontal cortex (mPFC) and dorsal hippocampus (dHIP) in adolescence. Representative immunoblot images for mPFC and dHIP are shown in A and E, respectively. The relative changes in the ratio of pGSK3β-Y216 to t-GSK3β, the ratio of pGSK3β-S9 to t-GSK3β, and the expression of t-GSK3β in the mPFC (B–D) and dHIP (F–H) were analyzed. LiCl pretreatment significantly inhibited the METH exposure-induced increase in the ratio of pGSK3β-Y216 to t-GSK3β in the dHIP (F) and decreased the ratio of pGSK3β-Ser9 to t-GSK3β in the mPFC (C) and dHIP (G) in adolescence. Data are expressed as the mean ± SEM; n = 10/group; *$P < .05$ and **$P < .01$, compared with the saline × saline group; #$P < .05$ and ##$P < .01$, comparison between the 2 indicated groups; 2-way ANOVA followed by the Bonferroni post hoc test.

more active than the control mice (saline × saline) ($P < .01$) and adolescent LiCl-pretreated and METH-exposed mice (LiCl × METH) ($P < .05$) (Figure 4B).

All the tested animals showed similar characteristics in the EPM test (Figure 4C,D; supplementary Table 1) and the 3rd day of the SPT (Figure 4E,F; supplementary Table 1).

Regarding the novel spatial exploration test, 2-way ANOVA for the data of the time spent (%) and latency to first entry in the novel arm revealed a significant effect of the interaction of METH exposure × LiCl pretreatment ($F_{(1,52)} = 15.58$, $P < .001$ and $F_{(1,52)} = 8.865$, $P < .01$, respectively), METH exposure ($F_{(1,52)} = 7.083$, $P < .05$ and $F_{(1,52)} = 7.236$, $P < .01$, respectively), and
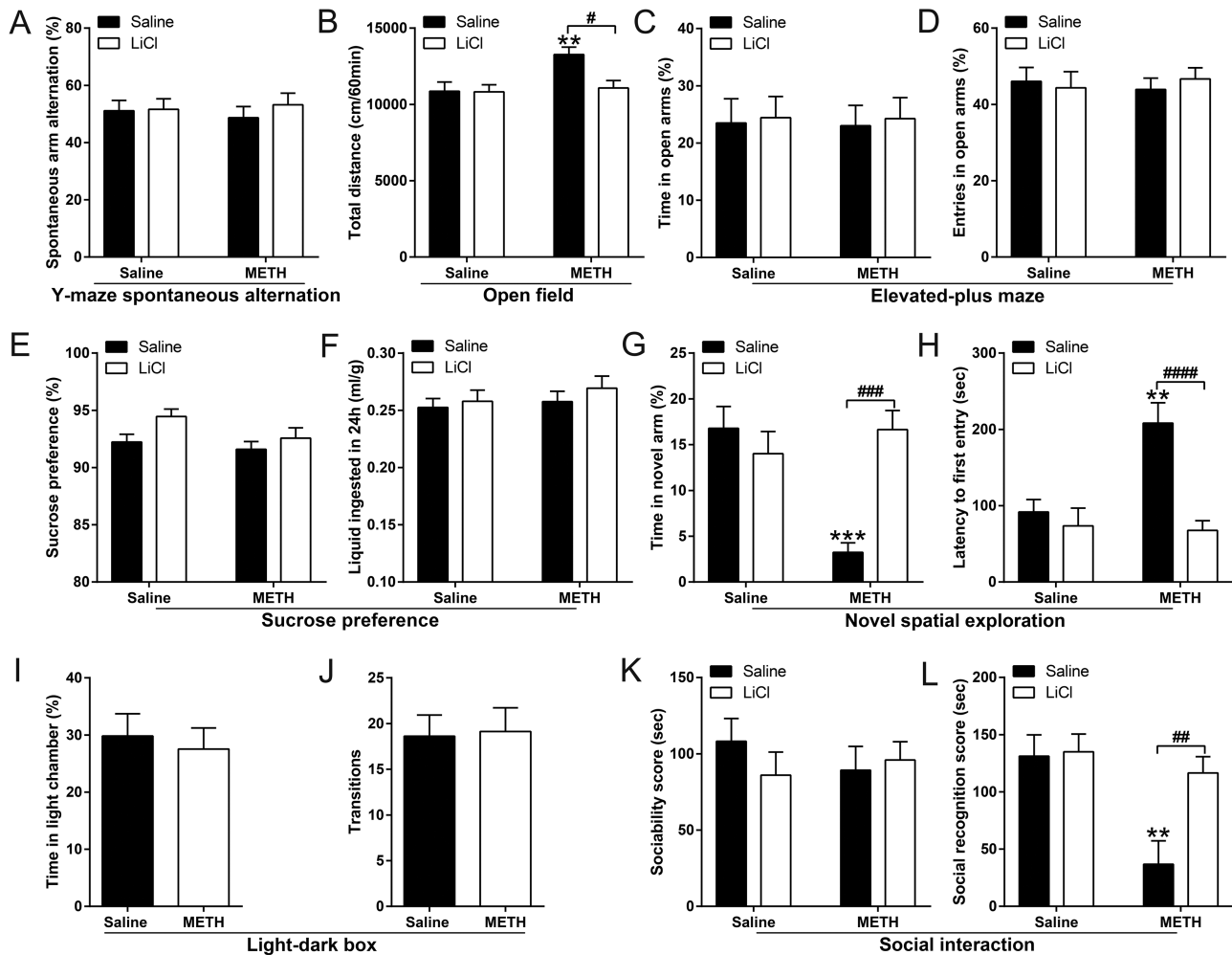
Figure 4. Effects of lithium chloride (LiCl) pretreatment on adolescent methamphetamine (METH) exposure-induced long-term alterations in emotion, cognition, and behavior in adulthood. Histograms show spontaneous arm alteration (%) in the Y-maze spontaneous alteration test (A), total distance moved in the open field test (OFT) (B), time spent and number of entries in the open arms (%) in the elevated-plus maze (EPM) test (C and D, respectively), sucrose preference (%) and total liquid ingested in the 3rd day of the sucrose preference test (SPT) (E and F, respectively), time spent (%) and latency to first entry in the novel arm in the novel spatial exploration test (G and H, respectively), time spent in the light chamber (%) and number of transitions in the light-dark box test (I and J, respectively), and the sociability scores and social recognition scores in the social interaction assay (K and L, respectively). Data are expressed as the mean ± SEM; n = 14/group (A–H, K and L), n = 8/group (I and J); **$P < .01$ and ***$P < .001$, compared with the saline × saline group; #$P < .05$, ##$P < .01$, ###$P < .001$ and ####$P < .0001$, comparison between the 2 indicated groups; 2-way ANOVA followed by the Bonferroni post hoc test (A–H, K and L), unpaired t tests (I and J).

LiCl pretreatment ($F_{(1,52)}$v6.713, $P < .05$ and $F_{(1,52)} = 14.95$, $P < .001$, respectively). Bonferonni's post hoc tests revealed that, in adulthood, saline × METH mice showed decreased time spent (%) and increased latency to first entry in the novel arm than did saline × saline mice ($P < .001$ and .01, respectively) and LiCl × METH mice ($P < .001$ and 0.0001, respectively) (Figure 4G,H). In addition, with the same withdrawal time in the novel spatial exploration test, adolescent saline- and METH-treated mice showed similar characteristics in the light-dark box test (Figure 4I,J).

For the sociability test, the results revealed that all tested animals showed similar sociability characteristics (Figure 4K; supplementary Table 1). However, for the social recognition memory test, 2-way ANOVA for the data of the social recognition score and the time spent in the novel chamber (%) revealed a significant effect of the interaction of METH exposure × LiCl pretreatment ($F_{(1,52)} = 4.727$, $P < .05$ and $F_{(1,52)} = 4.696$, $P < .05$, respectively), METH exposure ($F_{(1,52)} = 10.44$, $P < .01$ and $F_{(1,52)} = 10.63$, $P < .01$, respectively), and LiCl pretreatment ($F_{(1,52)} = 5.732$, $P < .05$ and $F_{(1,52)} = 6.643$, $P < .05$, respectively). Bonferonni's post hoc tests revealed that saline × METH mice obtained a lower average social

recognition score and decreased time spent in the novel chamber (%) than did saline × saline mice ($P < .01$ and .01, respectively) and LiCl × METH mice ($P < .01$ and .01, respectively) (Figure 4L; supplementary Table 1).

LiCl Pretreatment Prevented the Adolescent METH Exposure-Induced Long-Term Increase in GSK3β Activity in the dHIP in Adulthood

The results regarding the long-term effect of adolescent METH exposure on the activity of GSK3β in the mPFC and dHIP are shown in supplementary Figure 2 and Figure 5, respectively. We did not find any difference in the ratio of pGSK3β-Y216 to t-GSK3β or pGSK3β-Ser9 to t-GSK3β, the expression of t-GSK3β protein levels, or the distribution of pGSK3β-Ser9 in the mPFC among all 4 groups (supplementary Figure 2B–D, F). For the dHIP, western-blot analysis revealed no significant difference in the ratio of pGSK3β-Y216 to t-GSK3β or the expression of t-GSK3β protein levels among all 4 groups (Figure 5B,D), whereas 2-way ANOVA for the ratio of pGSK3β-Ser9 to t-GSK3β revealed a significant effect of the interaction of METH exposure × LiCl pretreatment

($F_{(1,28)}$ = 5.063, $P < .05$), METH exposure ($F_{(1,28)}$ = 4.450, $P < .05$) and LiCl pretreatment ($F_{(1,28)}$ = 5.544, $P < .05$). Bonferonni's post hoc tests revealed that, in adulthood, the ratio of pGSK3β-Ser9 to t-GSK3β was reduced by ~40% in saline × METH mice compared with that in control mice ($P < .05$) (Figure 5C). In addition, compared with saline × METH mice, LiCl × METH mice displayed a significant increase in the ratio of pGSK3β-Ser9/t-GSK3β ($P < .05$) (Figure 5C). Next, the immunochemical analysis was performed to compare the expression patterns and distribution of pGSK3β-Ser9 in the CA1, CA3, and DG subregions of the dHIP. Two-way ANOVA for the integrated optical density (IOD) of pGSK3β-Ser9 in CA1 and CA3 subregions revealed a significant effect of METH exposure ($F_{(1,8)}$ = 10.62, $P < .05$ and $F_{(1,8)}$ = 9.362, $P < .05$, respectively) and LiCl pretreatment ($F_{(1,8)}$ = 20.14, $P < .01$ and $F_{(1,8)}$ = 31.48, $P < .001$, respectively), but no interaction between METH exposure and LiCl pretreatment (Figure 5F,G).

LiCl Pretreatment Prevented the Adolescent METH Exposure-Induced Long-Term Decrease in Excitatory Synapse Density and Postsynaptic Density Thickness in the dHIP CA1 Subregion in Adulthood

Then, we further examined the ultrastructural changes in the excitatory synapses of the dHIP CA1, CA3, and DG subregions by using electron microscopy. For the CA1 subregion, electron microscopy revealed no significant differences in the width of synaptic cleft or the length of active zone (Figure 6D,E). However,

the 2-way ANOVA for the density of excitatory synapses and the thickness of PSD revealed a significant effect of the interaction of METH exposure × LiCl pretreatment ($F_{(1,8)}$ = 9.284, $P < .05$ and $F_{(1,8)}$ = 5.661, $P < .05$, respectively), METH exposure ($F_{(1,8)}$ = 37.14, $P < .001$ and $F_{(1,8)}$ = 9.016, $P < .05$, respectively), and LiCl pretreatment ($F_{(1,8)}$ = 18.95, $P < .01$ and $F_{(1,8)}$ = 10.46, $P < .05$, respectively). Bonferroni's post hoc tests revealed that, in adulthood, excitatory synapse density and PSD thickness in the CA1 subregion were reduced by approximately 30% and 15%, respectively, in saline × METH mice compared with those in control mice ($P < .01$ and $P < .05$, respectively) (Figure 6B,C). Additionally, compared with saline × METH mice, LiCl × METH mice displayed a significant increase in excitatory synapse density and PSD thickness in the CA1 subregion ($P < .01$ and $P < .05$, respectively) (Figure 6B,C). For the CA3 and DG subregions, there were no strong differences in the investigated structural parameters, including excitatory synapse density, PSD thickness, synaptic cleft width, or active zone length among all 4 groups (Figure 6F–M).

Experiment 4: METH Exposure Led to Alterations in Working Memory, Anxiety Behavior, and Novel Spatial Exploration in Adolescence

The most relevant results are shown in Figure 7 and the others are shown in supplementary Table 2. In adolescence, compared with saline-treated mice, METH-exposed mice showed
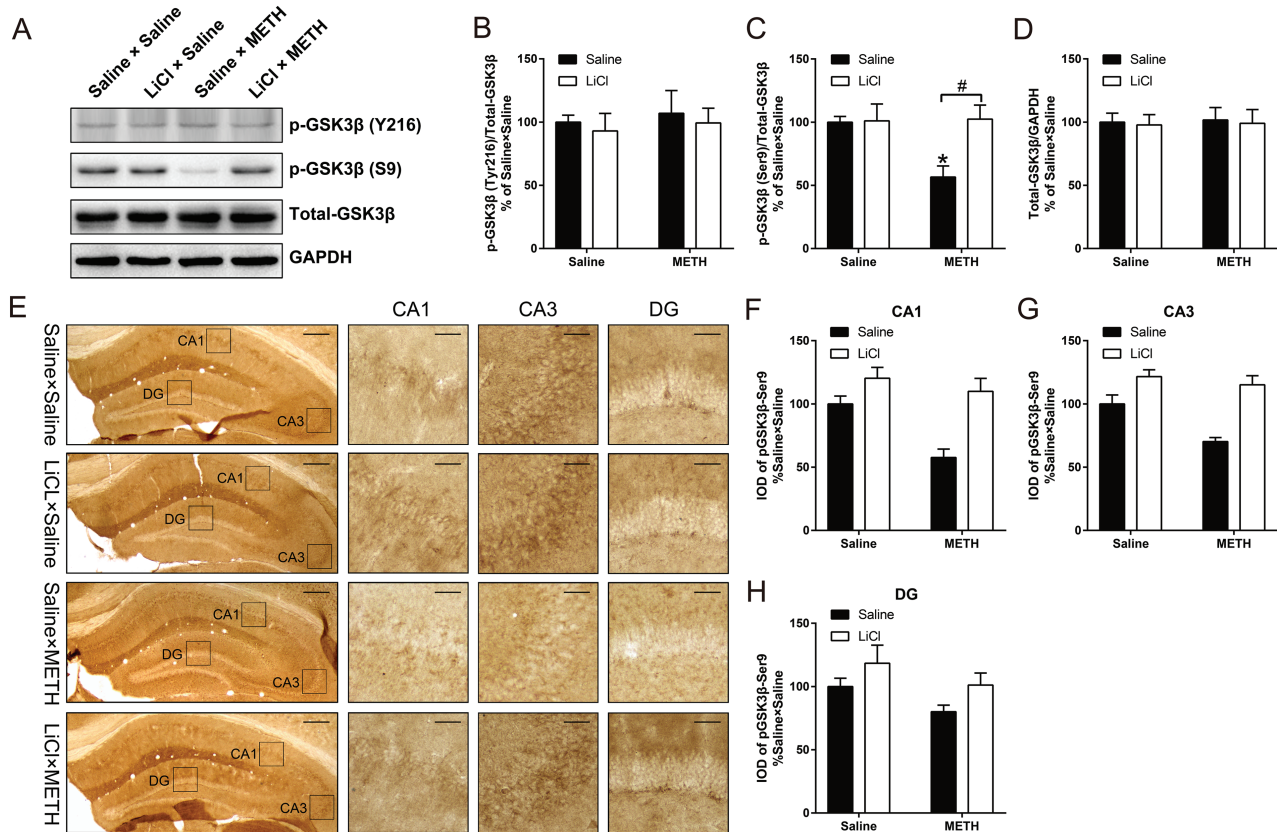

Figure 5. Effects of lithium chloride (LiCl) pretreatment on the abnormal activation of glycogen synthase kinase 3 beta (GSK3β) in the adult dorsal hippocampus (dHIP) induced by adolescent methamphetamine exposure. Representative immunoblot images are shown in A. The relative changes in the ratio of pGSK3β-Y216 to t-GSK3β (B), the ratio of pGSK3β-S9 to t-GSK3β (C), and the expression of t-GSK3β (D) were analyzed. Data are expressed as the mean ± SEM; n = 8/group; *P < .05 compared with the saline × saline group; #P < .05 comparison between the 2 indicated groups; Kruskal-Wallis tests (B), 2-way ANOVA followed by the Bonferroni post hoc test (C,D). Immunohistochemical analysis of pGSK3β-S9 immunoreactivity in the CA1, CA3, and dentate gyrus (DG) of the dHIP; the boxes indicate regions shown at higher magnification in the lower panels; scale bars represent 250 μm under low magnification and 50 μm under high magnification (E). The relative changes in the integrated optical density (IOD) of pGSK3β-Ser9 in CA1 (F), CA3 (G), and DG (H) were analyzed. Data are expressed as the mean ± SEM; n = 3/group; 2-way ANOVA.
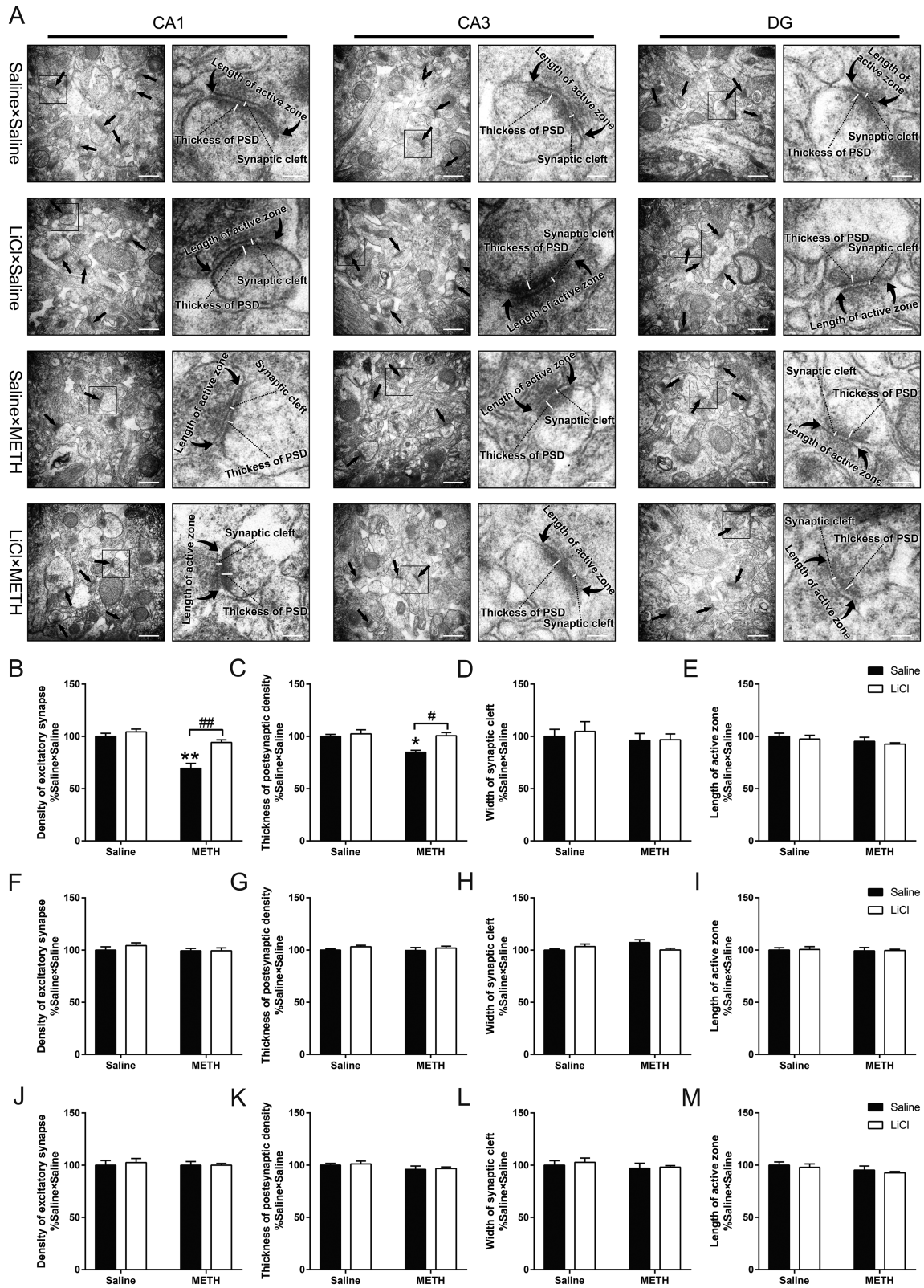
Figure 6. Effects of lithium chloride (LiCl) pretreatment on alterations in synaptic ultrastructure within different subregions of the adult dorsal hippocampus (dHIP) induced by adolescent methamphetamine (METH) exposure. Representative electron micrographs of the CA1, CA3, and dentate gyrus (DG) of the tested mice; the straight arrows indicate Gray's type-1 asymmetric synapses (excitatory synapses), whereas the curved arrows indicate the length of the presynaptic active zone; the boxes indicate regions shown at higher magnification in the lower panels, and scale bars represent 500 nm under low magnification and 100 nm under high magnification (A). Histograms show relative changes in the total number of excitatory synapses, thickness of postsynaptic density (PSD) at the thickest part, width of the synaptic cleft, and length of the active zone in CA1 (B–E), CA3 (F–I), and DG (J–M). More than 60 randomly chosen excitatory synapses from each subregion were analyzed. Data are expressed as the mean ± SEM; n = 3/group; *P < .05 and **P < .01, compared with the saline × saline group; #P < .05 and ##P < .01, comparison between the 2 indicated groups; 2-way ANOVA followed by the Bonferroni post hoc test.

decreased spontaneous alternation (%) in the Y-maze spontane-ous alternation test ($t_{(18)}$ = 2.533, P < .05) (Figure 7A), decreased time spent and number of entries in the open arms (%) in the EPM test ($t_{(17)}$ = 2.360, P < .05 and $t_{(17)}$ = 2.727, P < .05, respectively) (Figure 7C,D), and decreased time spent (%) and longest single visiting time in the novel arm in the novel spatial exploration test ($t_{(18)}$ = 2.781, P < .05 and $t_{(18)}$ = 2.717, P < .05, respectively) (Figure 7G,H). All tested mice displayed similar characteristics in the OFT, SPT, and social interaction assays (Figure 7; supple-mentary Table 2).

Adult METH Exposure Led to Long-Term Alterations in Social Recognition Memory but Not Locomotor Activity or Novel Spatial Exploration

The most relevant results are shown in Figure 8 and the others are shown in supplementary Table 3. Following long-term drug abstinence, adult METH-exposed mice showed a lower average social recognition score and decreased time spent in the novel chamber (%) than did adult saline-treated mice in the social interaction assay ($t_{(17)}$ = 2.425, P < .05 and $t_{(17)}$ = 2.553, P < .05,
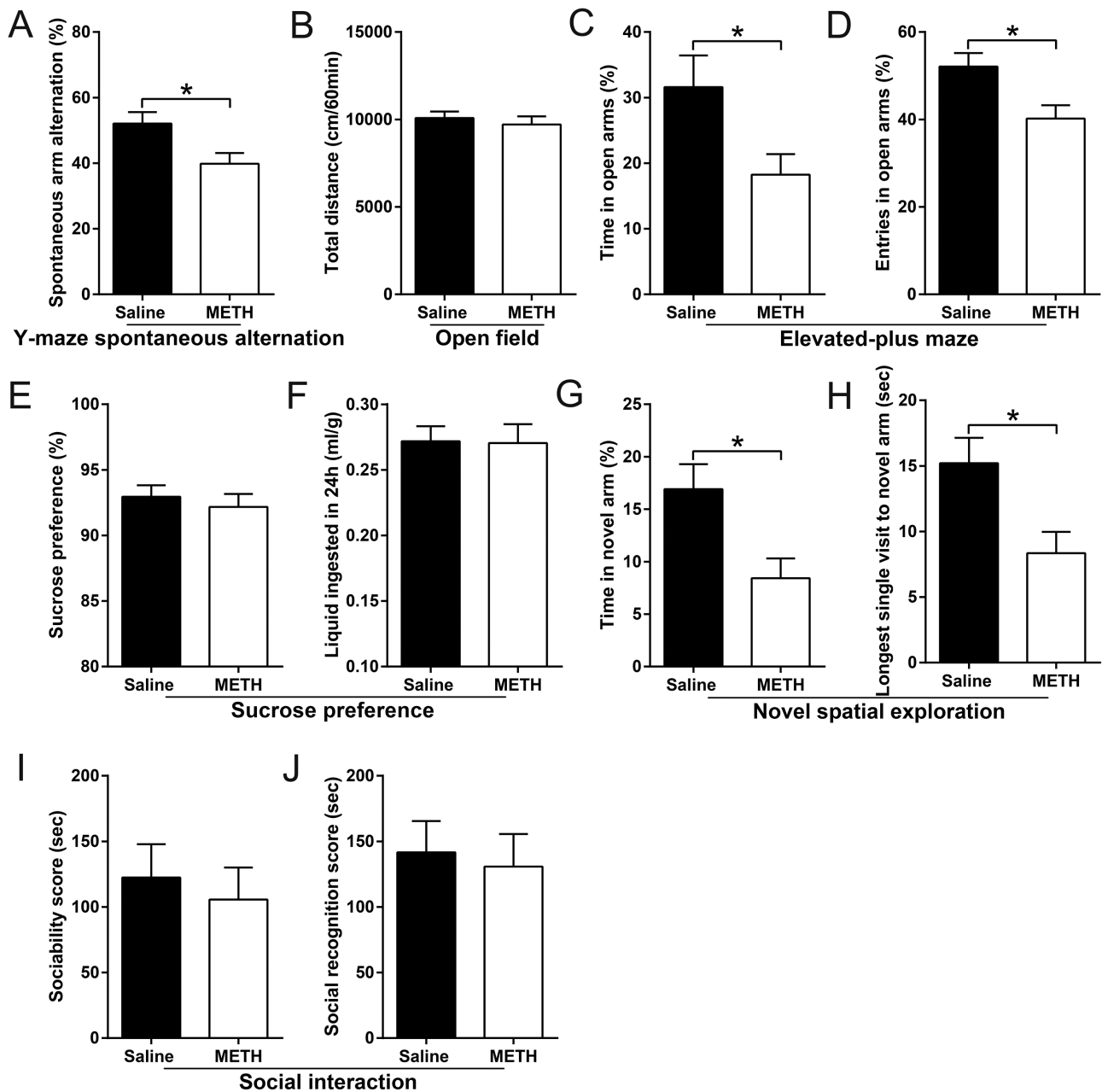

Figure 7. Effects of methamphetamine (METH) exposure on emotion, cognition, and behavior in adolescence. Histograms show spontaneous arm alteration (%) in the Y-maze spontaneous alternation test (A), total distance moved in the open field test (OFT) (B), time spent and number of entries in the open arms (%) in the elevated-plus maze (EPM) test (C and D, respectively), sucrose preference (%) and total liquid ingested in the 3rd day of the sucrose preference test (SPT) (E and F, respectively), time spent (%) and longest single visiting time in the novel arm in the novel spatial exploration test (G and H, respectively), and the sociability scores and social recognition scores in the social interaction assay (I and J, respectively). Data are expressed as the mean ± SEM; n = 10/group; *P < .05, comparison between the 2 indicated groups; unpaired *t* tests.

respectively) (Figure 8C; supplementary Table 3). All tested mice displayed no significant differences in the OFT and novel spatial exploration test (Figure 8; supplementary Table 3).

Experiment 5: Adolescent METH-Exposed Mice Did Not Display METH-Induced Locomotor Sensitization after Long-Term Drug Abstinence

The results are shown in Figure 9, and we did not find any significant differences in the distance traveled in each interval time (Figure 9A) or in total (Figure 9B) between the METH and saline groups.

Discussion

In the present study, we demonstrated the protective effects of pretreatment with LiCl on adolescent METH exposure-induced long-term alterations in behaviors and hippocampal ultrastructure in adults.

Adolescent METH exposure can induce emotional, behavioral, and cognitive deficits, but not all the deficits last for a long time (Hayase et al., 2005; McGregor et al., 2005; Haidar et al., 2016; Fonseca et al., 2017; Thompson et al., 2017). Based on our results, adolescent METH exposure-induced working memory deficits in the Y-maze spontaneous alternation test and anxiety-like behavior in the EPM test spontaneously recovered after long-term METH abstinence; reduced novel spatial exploration was observed both in adolescence and subsequent adulthood; and mild hyperactivity and impaired social recognition memory were found only in subsequent adulthood. In addition, adult METH exposure also led to long-term social recognition memory impairment. Further studies are needed to confirm these results. In addition, we did not observe METH-induced locomotor sensitization after 80 days of drug abstinence (Good and Radcliffe, 2011). This may be due to the fact that the mice were only received METH injection for 1 week and only with 1 mg/kg in adolescence in our locomotor sensitization test.

Our novel spatial exploration test was adapted from the Y-maze forced alternation test, which was used to detect novelty exploration and recognition memory (Dellu et al., 2000; Melnikova et al., 2006; Wolf et al., 2016). In contrast to previous studies, to increase recognition and navigation in the novel space, we marked the wall of the novel arm with a black and white pattern that was entirely different from the other 2 arms (Dellu et al., 2000; Melnikova et al., 2006; Wolf et al., 2016). If the 3 arms are the same (3 arms with no differences or mice have impaired spatial memory), mice could explore all arms equally (Dellu et al., 2000). Here, the average time spent in the novel arm (%) in each group was less than one-third, indicating that animals avoided the novel arm. Thus, our novel spatial exploration test may reflect anxiety more than memory. However, the changes in the EPM test spontaneously recovered after long-term METH abstinence. We further performed a light-dark box test to detect possible anxiety behavior, and no group differences were detected. Explaining the differences between these behavioral results is difficult, perhaps because different behavioral tests assess different anxiety profiles. In any case, adolescent METH exposure led to alterations in novel spatial exploration in adulthood.

Novel spatial exploration and social interaction behaviors critically depend on the intact function of the mPFC and dHIP, which are also vital for locomotion (Thinus-Blanc et al., 1996; Dellu et al., 2000; Adams et al., 2009; Casanova et al., 2013; Tanimizu et al., 2017). Our western-blot analysis in these brain regions indicates that adolescent METH exposure increases GSK3β activity by regulating the phosphorylated pattern of GSK3β. Specifically, S9-phosphorylated GSK3β (inhibitory form) rather than Y216-phosphorylated GSK3β (active form) contributed to the adolescent METH exposure-induced increase GSK3β activity in the mPFC, and this increased activity can be diminished with development. GSK3β activity in the mPFC showed almost no fluctuations from PND 45 to PND 51 (Xing et al., 2016). Therefore, we hypothesize that the relatively stable GSK3β activity is temporarily affected by METH exposure but would recover with METH abstinence. Regarding the dHIP, the adolescent METH exposure-induced increase in GSK3β activity was observed in adolescence and remained in adulthood (80 days after METH exposure, PND 132). S9-phosphorylated GSK3β (inhibitory form) may play a more important role in adolescent METH exposure-induced long-term deficits than does Y216-phosphorylated GSK3β (active form) in the dHIP. Compared with Y216-phosphorylated GSK3β, S9-phosphorylated GSK3β showed large fluctuations in its activity levels from PND45 to PND 51 in the dHIP (Beurel et al., 2012). METH exposure during this period could significantly disturb the developmental change in S9-phosphorylated GSK3β, which may result in a long-term
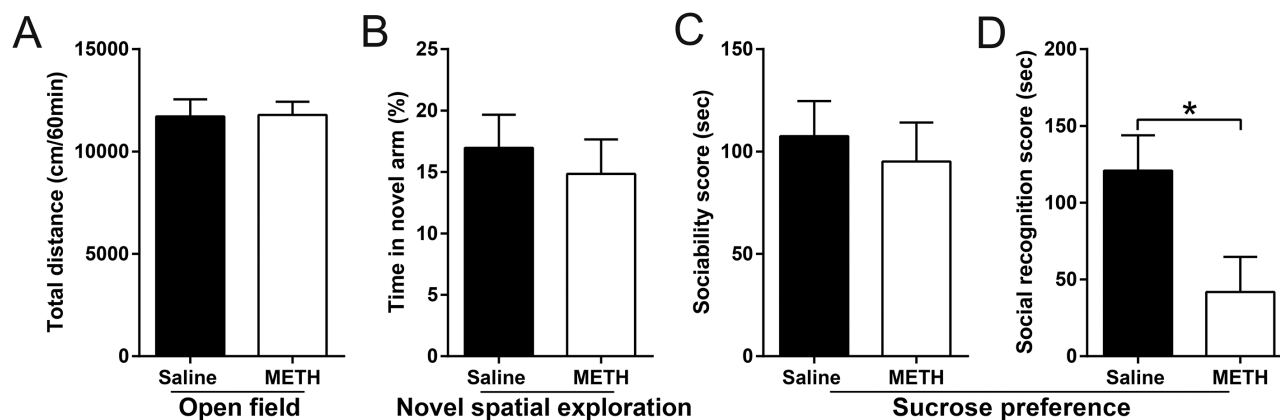

Figure 8. Effects of adult methamphetamine (METH) exposure on the locomotor activity, novel spatial exploration, and social interaction after long-term methamphetamine abstinence. Histograms show total distance moved in the open field test (OFT) (A), time spent in the novel arm (%) in the novel spatial exploration test (B), and the sociability scores and social recognition scores in the social interaction assay (C and D, respectively). Data are expressed as the mean ± SEM; n = 10/group; *P < .05, comparison between the 2 indicated groups; unpaired t tests.
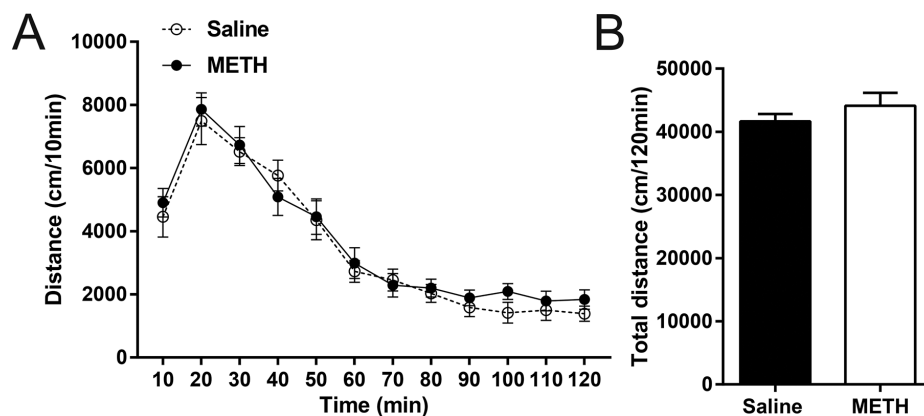
Figure 9. Effects of adolescent methamphetamine (METH) exposure on the expression of METH-induced locomotor sensitization in adulthood. All tested mice showed similar distance traveled at each interval (A) and in total (B). Data are expressed as the mean ± SEM; n = 8/group; 2-way ANOVA (A), unpaired *t* tests (B).

change in GSK3β activity in dHIP. In addition, the alteration in expression of S9-phosphorylated GSK3β was prominent in the CA1 and CA3 subregions of the dHIP, but the changes in synaptic ultrastructure were limited to the CA1 subregion. These results suggest that adolescent METH exposure-induced long-term dHIP damage is predominately located in the CA1 subregion and support that hyperactivation of GSK3β causes significant changes in synaptic plasticity (Salcedo-Tello et al., 2011; Nelson et al., 2013). METH exposure can attenuate brain tissue oxygen pressure, which often induces delayed neuronal damage (Kousik et al., 2011; Weaver et al., 2014). Additionally, among the various brain regions, the hippocampus is more vulnerable to hypoxia, especially in the CA1 subregion, but the DG subregion is relatively resistant (Gorter et al., 1997; Ouyang et al., 2007; Zhu et al., 2012). These reasons may explain why the CA1 subregion is more vulnerable to adolescent METH exposure-induced long-term hippocampal damage.

LiCl has neuroprotective effects, and more direct evidence indicates that LiCl attenuates METH-induced neurotoxicity and behavioral sensitization (Phiel and Klein, 2001; Xu et al., 2011; Wu et al., 2015). However, to the best of our knowledge, no study has investigated the potential role of LiCl in response to adolescent METH exposure-induced long-term consequences. In the present study, pretreatment with LiCl ameliorated adolescent METH exposure-induced mild hyperactivity, reduced novel spatial exploration, impaired social recognition memory, and increased GSK3β activity and changes in synaptic ultrastructure in the dHIP in adulthood. These results extend the findings of previous studies and indicate that LiCl can produce neuroprotection to resist adolescent METH exposure-induced long-term deficits (Phiel and Klein, 2001).

Our study has 3 limitations that must be addressed. First, the alterations in molecular and synaptic plasticity may not perfectly reflect behavioral alterations. Second, lithium directly inhibits GSK3α and GSK3β. The effect of GSK3α cannot be eliminated in our present study. Third, only one cognitive test was included in our present study. Thus, investigating other aspects of cognition function is necessary in future studies.

This study reveals that GSK3β is a key factor in adolescent chronic METH exposure-induced behavioral impairments. The CA1 region is more vulnerable to adolescent METH exposure. In addition, pretreatment with LiCl produced neuroprotection to prevent adolescent METH exposure-induced alterations in behavior and hippocampal ultrastructure in adulthood.

Furthermore, our study suggests that preventing dysregulation of GSK3β activity may be beneficial for adult individuals who are suffering from behavioral dysfunction induced by adolescent chronic METH exposure.

Supplementary Materials

Supplementary data are available at *International Journal of Neuropsychopharmacology (IJNPPY)* online.

Funding

Acknowledgments

Interest Statement

None.

References

Adams W, Ayton S, van den Buuse M (2009) Serotonergic lesions of the dorsal hippocampus differentially modulate locomotor hyperactivity induced by drugs of abuse in rats: implications for schizophrenia. Psychopharmacology (Berl) 206:665–676.

Beaulieu JM, Sotnikova TD, Yao WD, Kockeritz L, Woodgett JR, Gainetdinov RR, Caron MG (2004) Lithium antagonizes dopamine-dependent behaviors mediated by an AKT/glycogen synthase kinase 3 signaling cascade. Proc Natl Acad Sci U S A 101:5099–5104.

Beurel E, Mines MA, Song L, Jope RS (2012) Glycogen synthase kinase-3 levels and phosphorylation undergo large fluctuations in mouse brain during development. Bipolar Disord 14:822–830.

Brust V, Schindler PM, Lewejohann L (2015) Lifetime development of behavioural phenotype in the house mouse (Mus musculus). Front Zool 12(Suppl 1):S17.

Buck JM, Siegel JA (2015) The effects of adolescent methamphetamine exposure. Front Neurosci 9:151.

Casanova JP, Velis GP, Fuentealba JA (2013) Amphetamine loco-motor sensitization is accompanied with an enhanced high K+-stimulated dopamine release in the rat medial prefrontal cortex. Behav Brain Res 237:313–317.

Chen PC, Lao CL, Chen JC (2007) Dual alteration of limbic dopamine D1 receptor-mediated signalling and the Akt/GSK3 pathway in dopamine D3 receptor mutants during the development of methamphetamine sensitization. J Neurochem 100:225–241.

Dellu F, Contarino A, Simon H, Koob GF, Gold LH (2000) Genetic differences in response to novelty and spatial memory using a two-trial recognition task in mice. Neurobiol Learn Mem 73:31–48.

Fonseca R, Carvalho RA, Lemos C, Sequeira AC, Pita IR, Carvalho F, Silva CD, Prediger RD, Jarak I, Cunha RA, Fontes Ribeiro CA, Köfalvi A, Pereira FC (2017) Methamphetamine induces anhedonic-like behavior and impairs frontal cortical energetics in mice. CNS Neurosci Ther 23:119–126.

Good RL, Radcliffe RA (2011) Methamphetamine-induced loco-motor changes are dependent on age, dose and genotype. Pharmacol Biochem Behav 98:101–111.

Gorter JA, Petrozzino JJ, Aronica EM, Rosenbaum DM, Opitz T, Bennett MV, Connor JA, Zukin RS (1997) Global ischemia induces downregulation of Glur2 mRNA and increases AMPA receptor-mediated ca2+ influx in hippocampal CA1 neurons of gerbil. J Neurosci 17:6179–6188.

Haidar M, Lam M, Chua BE, Smith CM, Gundlach AL (2016) Sensitivity to chronic methamphetamine administration and withdrawal in mice with relaxin-3/RXFP3 deficiency. Neurochem Res 41:481–491.

Hayase T, Yamamoto Y, Yamamoto K (2005) Persistent anxiogenic effects of a single or repeated doses of cocaine and methamphetamine: interactions with endogenous cannabinoid receptor ligands. Behav Pharmacol 16:395–404.

Jalbrzikowski M, Larsen B, Hallquist MN, Foran W, Calabro F, Luna B (2017) Development of white matter microstructure and intrinsic functional connectivity between the amygdala and ventromedial prefrontal cortex: associations with anxiety and depression. Biol Psychiatry 82:511–521.

Kamei H, Nagai T, Nakano H, Togan Y, Takayanagi M, Takahashi K, Kobayashi K, Yoshida S, Maeda K, Takuma K, Nabeshima T, Yamada K (2006) Repeated methamphetamine treatment impairs recognition memory through a failure of novelty-induced ERK1/2 activation in the prefrontal cortex of mice. Biol Psychiatry 59:75–84.

King MK, Pardo M, Cheng Y, Downey K, Jope RS, Beurel E (2014) Glycogen synthase kinase-3 inhibitors: rescuers of cognitive impairments. Pharmacol Ther 141:1–12.

Kishimoto M, Ujike H, Okahisa Y, Kotaka T, Takaki M, Kodama M, Inada T, Yamada M, Uchimura N, Iwata N, Sora I, Iyo M, Ozaki N, Kuroda S (2008) The Frizzled 3 gene is associated with methamphetamine psychosis in the Japanese population. Behav Brain Funct 4:37.

Klein PS, Melton DA (1996) A molecular mechanism for the effect of lithium on development. Proc Natl Acad Sci U S A 93:8455–8459.

Kousik SM, Graves SM, Napier TC, Zhao C, Carvey PM (2011) Methamphetamine-induced vascular changes lead to striatal hypoxia and dopamine reduction. Neuroreport 22:923–928.

Luikinga SJ, Kim JH, Perry CJ (2018) Developmental perspectives on methamphetamine abuse: exploring adolescent vulnerabilities on brain and behavior. Prog Neuropsychopharmacol Biol Psychiatry 87:78–84.

McGregor C, Srisurapanont M, Jittiwutikarn J, Laobhripatr S, Wongtan T, White JM (2005) The nature, time course and severity of methamphetamine withdrawal. Addiction 100:1320–1329.

Melnikova T, Savonenko A, Wang Q, Liang X, Hand T, Wu L, Kaufmann WE, Vehmas A, Andreasson KI (2006) Cycloxygenase-2 activity promotes cognitive deficits but not increased amyloid burden in a model of Alzheimer's disease in a sex-dimorphic pattern. Neuroscience 141:1149–1162.

Moszczynska A, Callan SP (2017) Molecular, behavioral, and physiological consequences of methamphetamine neurotoxicity: implications for treatment. J Pharmacol Exp Ther 362:474–488.

Nelson CD, Kim MJ, Hsin H, Chen Y, Sheng M (2013) Phosphorylation of threonine-19 of PSD-95 by GSK-3β is required for PSD-95 mobilization and long-term depression. J Neurosci 33:12122–12135.

North A, Swant J, Salvatore MF, Gamble-George J, Prins P, Butler B, Mittal MK, Heltsley R, Clark JT, Khoshbouei H (2013) Chronic methamphetamine exposure produces a delayed, long-lasting memory deficit. Synapse 67:245–257.

Ouyang YB, Voloboueva LA, Xu LJ, Giffard RG (2007) Selective dysfunction of hippocampal CA1 astrocytes contributes to delayed neuronal damage after transient forebrain ischemia. J Neurosci 27:4253–4260.

Phiel CJ, Klein PS (2001) Molecular targets of lithium action. Annu Rev Pharmacol Toxicol 41:789–813.

Renard J, Rosen LG, Loureiro M, De Oliveira C, Schmid S, Rushlow WJ, Laviolette SR (2017) Adolescent cannabinoid exposure induces a persistent sub-cortical hyper-dopaminergic state and associated molecular adaptations in the prefrontal cortex. Cereb Cortex 27:1297–1310.

Salcedo-Tello P, Ortiz-Matamoros A, Arias C (2011) GSK3 function in the brain during development, neuronal plasticity, and neurodegeneration. Int J Alzheimers Dis 2011:189728.

Smith RF (2003) Animal models of periadolescent substance abuse. Neurotoxicol Teratol 25:291–301.

Spear LP (2016) Consequences of adolescent use of alcohol and other drugs: studies using rodent models. Neurosci Biobehav Rev 70:228–243.

Tanimizu T, Kenney JW, Okano E, Kadoma K, Frankland PW, Kida S (2017) Functional connectivity of multiple brain regions required for the consolidation of social recognition memory. J Neurosci 37:4103–4116.

Thinus-Blanc C, Save E, Rossi-Arnaud C, Tozzi A, Ammassari-Teule M (1996) The differences shown by C57BL/6 and DBA/2 inbred mice in detecting spatial novelty are subserved by a different hippocampal and parietal cortex interplay. Behav Brain Res 80:33–40.

Thompson AB, Gerson J, Stolyarova A, Bugarin A, Hart EE, Jentsch JD, Izquierdo A (2017) Steep effort discounting of a preferred reward over a freely-available option in prolonged methamphetamine withdrawal in male rats. Psychopharmacology (Berl) 234:2697–2705.

Tian Y, Wang Y, Deng Y, Maeda K (2009) Methylphenidate improves spatial memory of spontaneously hypertensive rats: evidence in behavioral and ultrastructural changes. Neurosci Lett 461:106–109.

UNODC (2017) World drug report 2017. New York.

Vorhees CV, Reed TM, Morford LL, Fukumura M, Wood SL, Brown CA, Skelton MR, McCrea AE, Rock SL, Williams MT (2005) Periadolescent rats (P41-50) exhibit increased susceptibility to D-methamphetamine-induced long-term spatial and sequential learning deficits compared to juvenile (P21-30 or P31-40) or adult rats (P51-60). Neurotoxicol Teratol 27:117–134.

Wang J, Sun LL, Zhu WL, Sun Y, Liu JF, Lu L, Shi J (2012) Role of calcineurin in the VTA in rats behaviorally sensitized to methamphetamine. Psychopharmacology (Berl) 220: 117–128.

Wang Y, Yin F, Guo H, Zhang J, Yan P, Lai J (2017) The role of dopamine D1 and D3 receptors in N-methyl-D-aspartate (NMDA)/glycineb site-regulated complex cognitive behaviors following repeated morphine administration. Int J Neuropsychopharmacol 20:562–574.

Weaver J, Yang Y, Purvis R, Weatherwax T, Rosen GM, Liu KJ (2014) In vivo evidence of methamphetamine induced attenuation of brain tissue oxygenation as measured by EPR oximetry. Toxicol Appl Pharmacol 275:73–78.

Wierenga L, Langen M, Ambrosino S, van Dijk S, Oranje B, Durston S (2014) Typical development of basal ganglia, hippocampus, amygdala and cerebellum from age 7 to 24. Neuroimage 96:67–72.

Wolf A, Bauer B, Abner EL, Ashkenazy-Frolinger T, Hartz AM (2016) A comprehensive behavioral test battery to assess learning and memory in 129S6/Tg2576 mice. Plos One 11:e0147733.

Wu J, Zhu D, Zhang J, Li G, Liu Z, Sun J (2015) Lithium protects against methamphetamine-induced neurotoxicity in PC12 cells via Akt/GSK3β/mtor pathway. Biochem Biophys Res Commun 465:368–373.

Xing B, Liang XP, Liu P, Zhao Y, Chu Z, Dang YH (2015) Valproate inhibits methamphetamine induced hyperactivity via glycogen synthase kinase 3β signaling in the nucleus accumbens core. Plos One 10:e0128068.

Xing B, Li YC, Gao WJ (2016) GSK3β hyperactivity during an early critical period impairs prefrontal synaptic plasticity and induces lasting deficits in spine morphology and working memory. Neuropsychopharmacology 41:3003–3015.

Xu CM, Wang J, Wu P, Xue YX, Zhu WL, Li QQ, Zhai HF, Shi J, Lu L (2011) Glycogen synthase kinase 3β in the nucleus accumbens core is critical for methamphetamine-induced behavioral sensitization. J Neurochem 118:126–139.

Zhu H, Yoshimoto T, Imajo-Ohmi S, Dazortsava M, Mathivanan A, Yamashima T (2012) Why are hippocampal CA1 neurons vulnerable but motor cortex neurons resistant to transient ischemia? J Neurochem 120:574–585.